Arctic, Antarctic, and Alpine Research, Vol. 34, No. 2, 2002, pp. 150–158

Ice Formation in an Antarctic Glacier-dammed Lake and Implications for Glacier-Lake Interactions

*R. Lorrain,**
*S. Sleewaegen,**
S. Fitzsimons,†
and M. Stiévenard‡

*Département des Sciences de la Terre, Université Libre de Bruxelles, CP 160/03, B-1050 Brussels, Belgium. rlorrain@ulb.ac.be
†Department of Geography, University of Otago, P.O. Box 56, Dunedin, New Zealand.
‡Laboratoire des Sciences du Climat et de l'Environnement, Laboratoire mixte CEA-CNRS-CE Saclay, F-91191 Gif-sur-Yvette Cedex, France.

Abstract

Perennially frozen lakes are common features in the McMurdo Dry Valleys of South Victoria Land in Antarctica. Some of them, called wet based, contain liquid water capped by a permanent ice cover between 2.5 and 6 m in thickness. The others, called dry based, are ice-block lakes. The thickness of the latter may far exceed those of the former. Their level is rising from freezing of the surface flooding of summer meltwater. However, we show here for the first time, using isotopic analyses together with an ionic and gas content and composition study, that the ice of one of these dry-based lakes has been formed by complete freezing from top to bottom of a closed water reservoir and not by successive layers of icings (aufeis) piling on top of each other. We also show how this lake, dammed by a cold-based glacier, has contributed to the formation of the basal ice layer of this glacier.

Introduction

The McMurdo Dry Valleys, a small group of ice-free areas situated along the coastal regions of South Victoria Land (Antarctica), are the settings for a series of closed-basin, permanently ice-covered lakes, some of which are dammed by local "alpine" glaciers.

Recently, three of us (Lorrain et al., 1999) examined the possible relationships between one of these ice-dammed lakes and its adjacent cold-based damming glacier (Lake Popplewell and Suess Glacier situated in the Taylor Valley—Fig. 1). We concluded (Lorrain et al., 1999), on ice composition grounds, that water from the lake has played a major role in the formation of the stacked sequence of ice and sediment layers accreted at the glacier base. This conclusion was shown to be consistent with a previously proposed model of debris entrainment by cold-based glaciers flowing into lakes (Fitzsimons, 1996). This model states that transient wet-based conditions occur as ice flows into the unfrozen sediments of the lake bottom, creating conditions favorable for the entrainment of sediments and for ice accretion by water freezing. However, our new fieldwork has allowed us to realize that the studied lake is frozen to its bed. The question of the origin of the liquid water considered in the model of debris entrainment has thus to be re-evaluated in that context. To this end, this paper focuses on the formation processes of the lake ice itself.

The Dry Valleys lakes have been the subject of many recently published papers. Extended reviews are available in two books, edited by Green and Friedman (1993) and by Priscu (1998). However, very few of the papers (and those cited therein) in these books are devoted to the ice cover; three exceptions are extensive studies by Chinn (1993), Adams et al. (1998), and Fritsen et al. (1998). Only the first of them deals with dry-based lakes. In particular, Chinn (1993) shows that dry-based lakes are the most common types found at higher altitudes than the "regional snowline" or away from the arid Dry Valleys area. However, he points out that Lake Vida (Victoria Valley) is an exception as it is well below the regional snowline. The present study is based on ice composition analyses. Stable isotopes (δD and $\delta^{18}O$), major ions, total gas content, and gas composition analyses were performed; ice textural and structural studies were also carried out. To our knowledge, such an investigation of lake ice from the Dry Valleys has never been reported.

Site Description and Methods

Lake Popplewell (unofficial name) is a relatively small, perennially frozen lake, about 350 m long and 150 m wide, dammed in Taylor Valley by Suess Glacier which descends on the northern slope of the valley and flows across its floor (Fig. 1). The lake surface, which is about 110 m a.s.l., appears bluish and very smooth, except in a few places were ice mounds are present. The latter are less than 1 m high, have a diameter of about 10 m, and present some shallow radial cracks. During the summer, a narrow moat (1.5 m of mean width) of liquid water appears mainly along the southern shore. This moat is even narrower along the northern shore because this side is more frequently in the shadow of the steep slope which dominates the valley; sometimes, the moat does not form on the northern side.

The lake ice was drilled during the summer (January 1998) at four locations with a SIPRE-type ice auger, 7.5 cm in diameter (Fig. 1). All drilling was stopped when the auger was not able to go deeper. In each case, the ice was in contact with frozen sediments which we consider to be the bottom sediments, indicating a dry-based lake. The ice thickness varies between 2.47 and 4.76 m. Borehole temperature, measured a few hours after coring, was never lower than −0.5°C. Liquid water was not encountered except in one case, in a pocket about 40 cm thick located at about 280 cm deep. Similar water pockets have been observed by Chinn (1993) and Fritsen et al. (1998) in the ice covering neighboring lakes (Lake Bonney and Lake Hoare—see Fig. 1).

Temperature loggers were used to monitor the ice cores from their initial storage in the field to their laboratory storage in Brussels; the temperature of the samples did not rise above −15°C. Once in Brussels, the samples were kept at −18°C.

1523-0430/02 $7.00

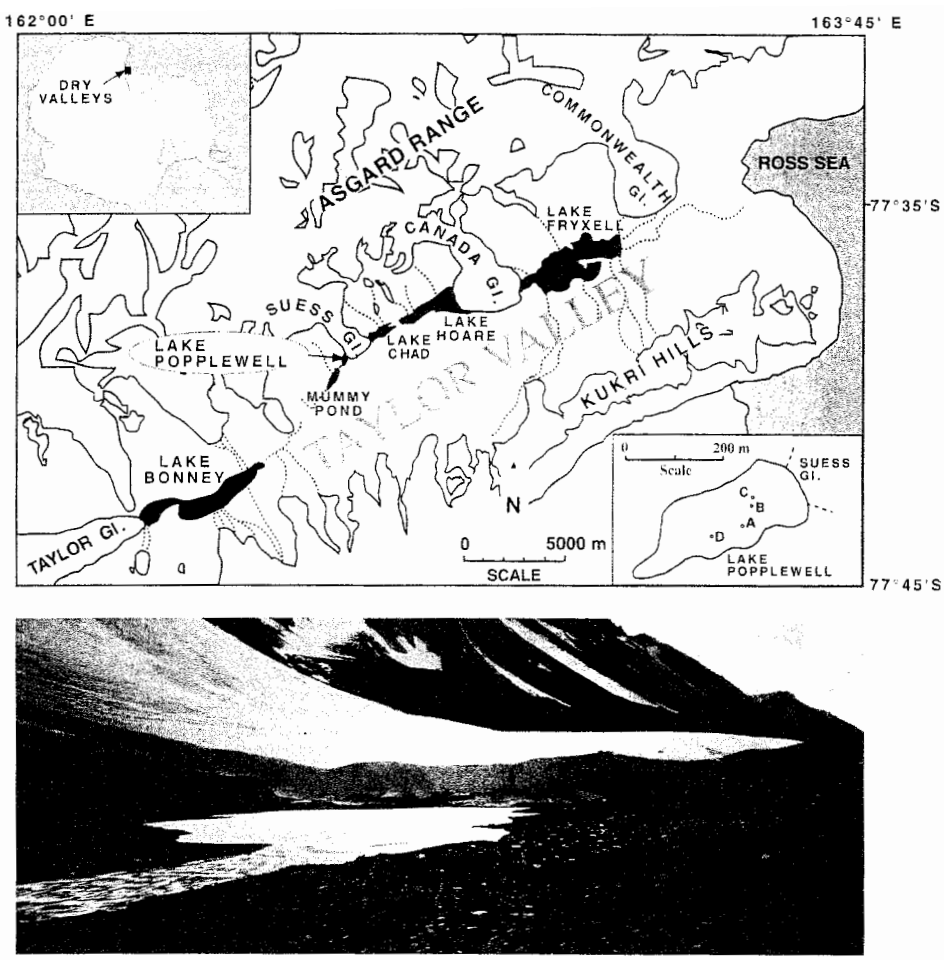

FIGURE 1. Top: Location map of the perennially frozen lakes of Taylor Valley (dotted lines represent meltstreams), with inset of Lake Popplewell showing coring sites. Bottom: Eastward view of Lake Popplewell with Suess Glacier in the background.

Close examination of the four cores was performed in the cold laboratory in Brussels. Longitudinal thin sections were cut all along the cores and photographed between crossed polaroids allowing ice-texture observations. It clearly appeared that the four cores were very similar except the basal part of the core A (Fig. 1) which is the longest (476 cm). Core A is the only one containing sediments layers a few centimeters thick interbedded with thicker ice bands. Because of this particular situation, this core will be the subject of another study devoted to sediment trapping by lake ice. In the present paper, we discuss the data obtained from the detailed sampling of core D.

The isotopic analyses were performed at the Nuclear Research Center of Saclay in France. Results are expressed in δ-units normalized to SMOW (Standard Mean Ocean Water). Precision of the measurements is ±0.5‰ on δD and ±0.1‰ on $\delta^{18}O$. All the other analyses were performed in Brussels. Na^+, K^+, Ca^{2+}, and Mg^{2+} were determined by atomic absorption spectrophotometry (Varian SpectrAA 300) with a precision of 3%. Cl^-, SO_4^{2-}, and NO_3^-, were determined by ionic chromatography (Dionex DX100 with conductimetric detector) with a precision of 5% for Cl^- and SO_4^{2-} for the concentration ranges encountered. NO_3^- was undetectible in most of our samples (detection limit = 0.2 ppm). Total gas content was determined by a melting-refreezing method using a Toepler pump. This method was fully described by Raynaud et al. (1988) and Blunier et al. (1993). The relative precision is better than 5% (Martinerie et al., 1994). Gas composition was measured using a dry extraction technique at −55°C in a cold room, using a Varian 3300 gas chromatograph. The procedure followed was fully described by Raynaud et al. (1982) and Barnola et al. (1983). The precision of the measurements is 2.5% for CO_2 and 0.4% for O_2 and N_2.

Results

Figure 2a shows the different ice types observed in one of the ice cores retrieved from the lake ice. This core, 331 cm long, is considered to be representative of the lake ice mass. It does not contain any water pockets or any visible mineral particles, except at its very bottom where the ice auger was able to obtain 1 cm of frozen sediments. From the surface to 35 cm depth, the ice was extremely brittle so that it was not possible to obtain a useful sample. Below this depth, the core shows columnar crystals, a few decimeter long (some of them reaching 1 m long), with vertical c-axes. This texture described as "candle ice" by Chinn and Maze (1983) is typical of lake ice. Cylindrical bubbles, 1 to 6 cm long and 1 to 3 mm wide, are present all along the core (Fig. 3a). These crystal and bubble characteristics indicate downward progression of a freezing front through a water mass (Gow and Langston, 1977). The bubbles are produced by occlusion of gas within the ice during freezing and are oriented along the direction of ice growth (Adams et al., 1998). Close observation of the core, in particular between 110 and 180 cm depths, reveals that the shapes of the bubbles are highly variable. Among others, one finds thin and sinuous cylindrical and sometimes dendritic bubbles less than 1 mm in diameter (Fig. 3b), thick and irregular cylindrical bubbles reaching 5 mm in diameter (Fig. 3c, d), and large, nearly spherical bubbles up to 10

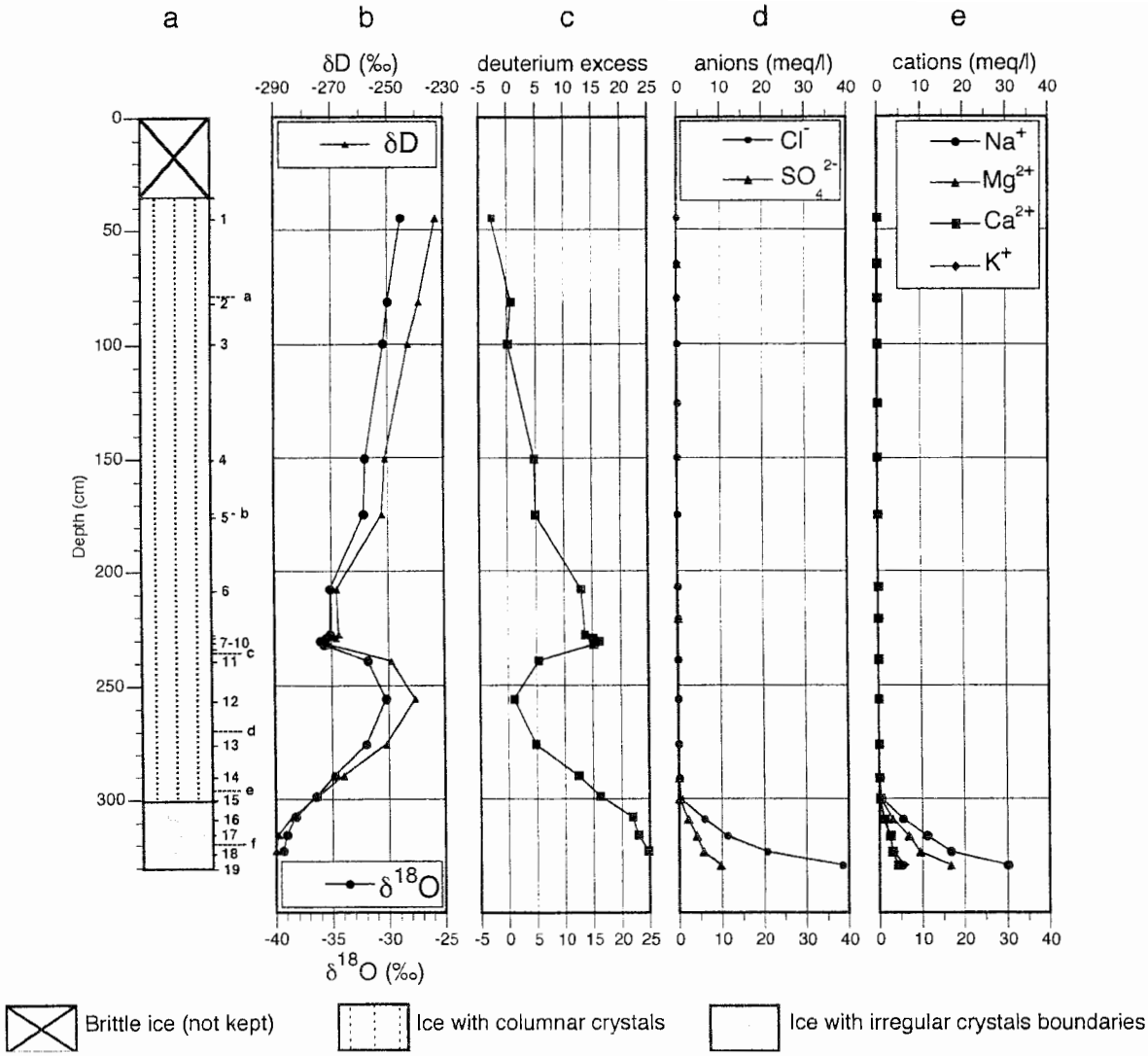

FIGURE 2. Main characteristics of core D: (a) types of ice with locations of the isotopic and chemical samples noted 1 to 19 and of samples for gaseous analyses noted a to f; (b) δD and $\delta^{18}O$ profiles in ‰; (c) deuterium excess profile; (d) major anions profiles (Cl^- SO_4^{2-} in meq L^{-1}); (e) major cations profiles (Na^+, K^+, Ca^{2+}, Mg^{2+}, in meq L^{-1}).

mm in diameter (Fig. 3b), similar to the "inverted teardrops" described by Adams et al. (1998).

In the bottom 30 cm of the core, the bubbles appear as vertically oriented filaments a few millimeters to 1 cm long and with a diameter of the order of a tenth of millimeters (Fig. 3e). The ice crystals are still vertically elongated, but with horizontal c-axes. However, in the last 10 cm, the ice crystals become relatively small (1 cm to a few centimeters long) with random c-axis orientation and with cylindrical bubbles situated along their boundaries (Fig. 3f, g). In horizontal thin section, each individual crystal shows irregular boundaries and evenly spaced ice plates and brine lamellae (Fig. 3h) which has been previously described in the case of certain types of sea ice as the "brine layer/ice plate substructure." This has been clearly illustrated by Gow et al. (1987). Moreover, small algal fragments are present within the last 1 cm of ice, and also in the frozen sediments which constitute the very end of the core.

The isotopic profile shows clear trends (Fig. 2b, c). The δD and $\delta^{18}O$ values become more negative with increasing depth indicating a depletion of heavy isotopes down to 230 cm. Below this depth, an inverse trend takes place until 256 cm where a new depletion is again displayed until the sediment is reached. Values are −232.8‰ in δD and −28.76‰ in $\delta^{18}O$ at the top of the profile and reach −290.0‰ and −39.33‰, respectively, near the bottom. The inverse trend detected between 230 and 256 cm deep represents quite smaller shifts, between −270.2 and −240.5‰ in δD and between −35.68 and −30.19‰ in $\delta^{18}O$. The deuterium excess profile ($d = \delta D - 8\ \delta^{18}O$) appears as a mirror image of the δ profiles.

The major ions profiles are simpler (Fig. 2d, e). All of them have relatively low concentrations all along the core except at its very bottom where they sharply rise, reaching higher values. Along the last 30 cm, chloride, the dominant anion, becomes 100 times more concentrated (from 0.39 to 38.49 meq L^{-1}) and sodium, the dominant cation, increases from 0.45 to 30.20 meq L^{-1}. The other ions analyzed exhibit the same trend but to a lesser extent.

Gas content and composition analyses were performed on six samples situated between 79 and 319 cm depth (Fig. 2a). Gas content is always low (it ranges from 0.019 to 0.080 cm^3 g^{-1}). This range is clearly related to the bubble concentration, but it must be noted that some bubbles are so large that sampling

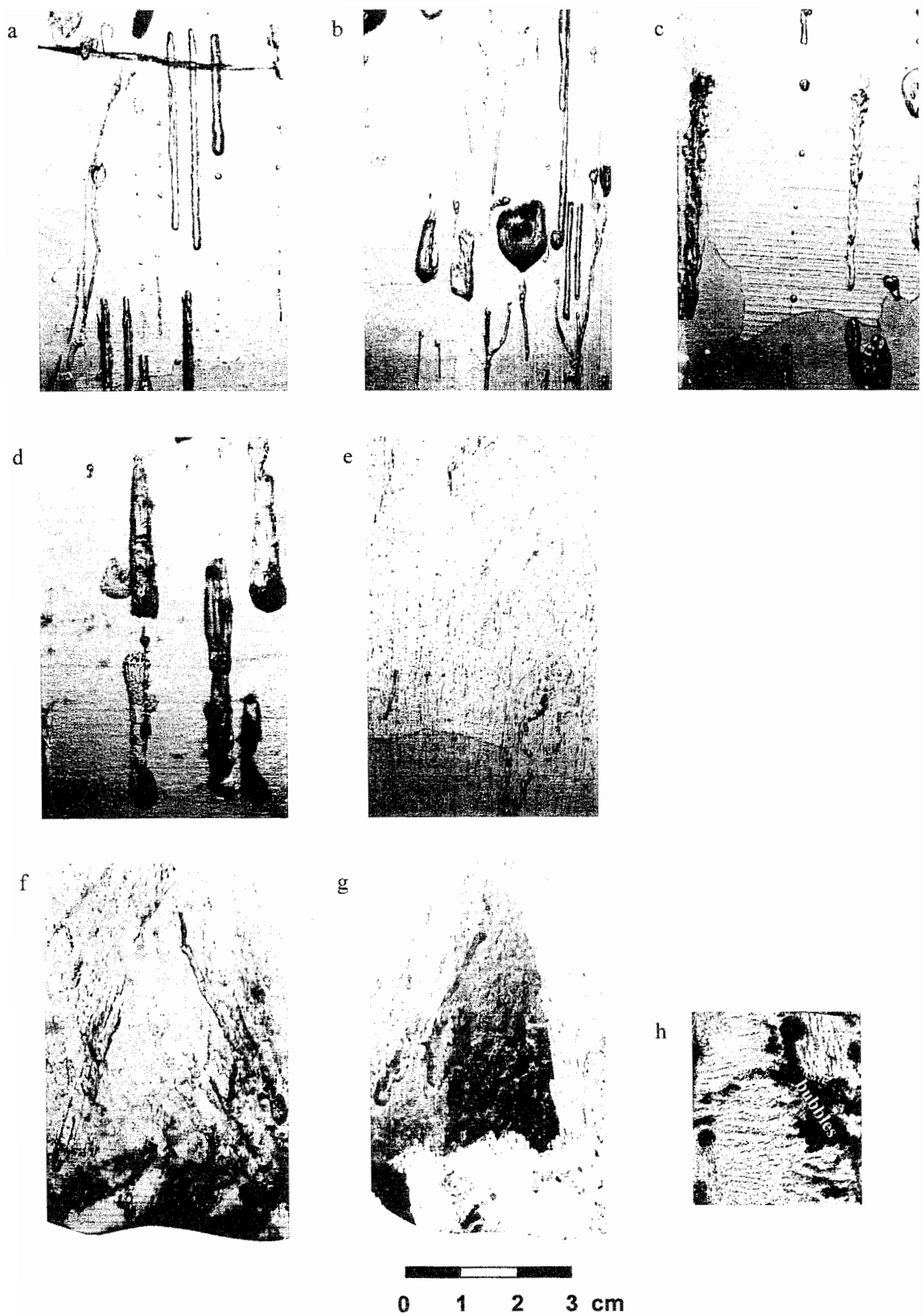

FIGURE 3. Bubbles shapes displayed in vertical sections along core D and substructure: (a) common vertical cylindrical bubbles; (b) thin sinuous, sometimes dendritic, cylindrical bubbles and big nearly spherical bubble similar to an inverted teardrop bubble; (c–d) thick and irregular cylindrical bubbles; (e) very thin vertically oriented bubbles, appearing like filaments; (f) cylindrical bubbles situated along crystals boundaries of smaller crystals visible in vertical thin section on (g); (h) horizontal thin section of the basal part of the core showing crystals with striated surfaces similar to the "brine-layer/ice plate substructure" developed in sea ice (Gow et al., 1987).

necessarily implies the cutting of them, and thus loss of gases. The CO_2 concentration is relatively low all along the core (between 564 and 4557 ppmv) contrasting with nearly 700.000 ppmv near the bottom. The O_2/N_2 ratio gradually increases from top to bottom from 0.37 to 0.54.

Discussion

ISOTOPIC DATA

When plotted on a $\delta D/\delta^{18}O$ diagram (Fig. 4), the 19 ice samples taken all along the ice core show a linear relationship expressed by the equation:

$$\delta D = 5.4\ \delta^{18}O - 77\ (r^2 = 0.99). \quad (1)$$

The slope of this regression line ($S = 5.4$), called freezing slope, is an isotopic signature of ice formed by progressive freezing of a closed water reservoir, as explained by Jouzel and Souchez (1982) and Souchez and Jouzel (1984). As the freezing front moves, ice is enriched in heavy isotopes with respect to water. In a closed or quasi-closed reservoir, the residual water becomes more and more depleted in heavy isotopes and the successive ice layers formed are therefore depleted in heavy isotopes as well. The slope depends on the isotopic composition of the water at the beginning of freezing and on the ice-water equilibrium fractionation coefficient for D and ^{18}O. The following equation from Souchez and Jouzel (1984) can be used to compute this slope:

$$S = \frac{\alpha[(\alpha - 1)(1 + \delta i)]}{\beta[(\beta - 1)(1 + \Delta i)]} \quad (2)$$

where δi is the δD composition of the parent water, Δi its $\delta^{18}O$ composition, and α and β are the values of the ice water equilibrium coefficients for deuterium and for ^{18}O, respectively (Souchez and Jouzel, 1984). The composition of the parent water, as suggested by Souchez and Jouzel (1984) is given by the intersection of the freezing slope with the local meteoric waterline. The latter has been obtained by Lorrain et al. (1999) from 25 glacier ice samples from the surface of Suess Glacier. These 25 samples have isotopic values ranging from −38.51 to −30.77‰ in $\delta^{18}O$ and from −307.4 to −248.6‰ in δD. Very few measurements were previously published for this glacier: −30.0 and −226‰ (Matsubaya et al., 1979), −30.4, −30.6, and −35.1‰ in $\delta^{18}O$ (Stuiver et al., 1981). Most of the values reported by Lorrain et al. (1999) are more negative. The meteoric water line they obtained has the following equation

$$\delta D = 8.1\ \delta^{18}O + 9.4\ (r^2 = 0.98). \quad (3)$$

The corresponding isotopic values of the parent water are $\delta^{18}O = -32.32‰$ and $\delta D = -252.38‰$. Using them as δi and Δi in equation (2) with α and β taken as 1.0208 and 1.003, respectively (Souchez and Jouzel, 1984), we obtain a theoretical freezing slope of 5.5 which is in close agreement with the slope of 5.4 obtained from our samples.

It is also possible to estimate the isotopic composition of the ice formed when the freezing front has reached the bottom of the water reservoir. In a closed system, what mass is gained by the solid phase during freezing is lost by the liquid phase. Therefore, as demonstrated by Jouzel and Souchez (1982),

$$\delta_S = \alpha(1000 + \delta_0)\left[\frac{N_0 - N_S}{N_0}\right]^{\alpha - 1} - 1000 \quad (4)$$

where N_0 is the total number of moles in the system or the number of moles in the liquid when freezing begins, N_S is the number of moles in the solid phase at time t, δ_s is the δ value of the solid phase near the liquid-solid interface at time t, δ_0 is the δ value of the solution when freezing begins, and α is the equilibrium fractionation coefficient between solid and liquid. From equation (4), we can estimate the δ values of the ice corresponding to a given frozen fraction (N_S/N_0). For instance, at 97% freezing, the corresponding isotopic composition is $\delta^{18}O = -39.57‰$ and $\delta D = -290.5‰$. These values are nearly the same as the ones of the deepest isotopic sample (see in Fig. 2, sample No. 18, 323 cm deep, $\delta^{18}O = -39.33‰$ and $\delta D = -290.0‰$).

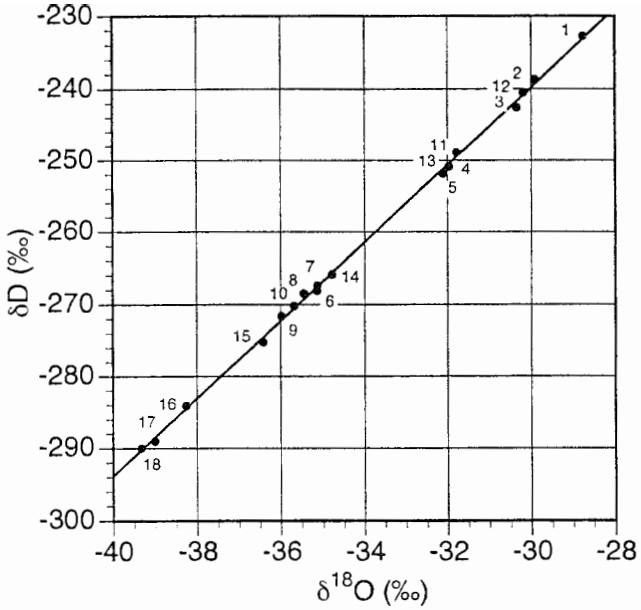

FIGURE 4. $\delta D/\delta^{18}O$ diagram showing the 18 samples located all along core D (see Fig. 2a).

Thus, isotopic results confirm that the lake ice studied was formed by progressive and complete freezing of the whole liquid water mass from top to bottom. However, between 230 and 256 cm depth, an enrichment in heavy isotopes with depth has been detected. This can be explained by mixing of the residual liquid water of the lake with water having higher isotopic values that plot onto the freezing slope cited above. Only on the latter condition can the isotopic values of the ice formed after mixing plot onto the same freezing slope (e.g., point 12 in Fig. 4). We think this mixing occurred when, during summer, the residual water situated at the lake bottom eventually made contact with moat water.

CHEMICAL DATA

The chemical results confirm the interpretation of the isotopic data. The ionic concentrations profile showing low values all along the ice core except at its bottom expresses the chemical effects of the migration of the freezing front. During downward freezing of the lake water, most ions are expelled from the ice and diffuse into the residual water (Terwilliger and Dizio, 1970; Hallet, 1976). Near the end of the closed reservoir the ionic concentration become very high and, as a result, rises in the ice as well. Finally as the freezing front becomes grounded, the last ice increments must include most of the expelled ions.

The high final ionic concentration of this ice, although weaker than in the case of sea ice, is responsible for the presence of the brine layer/ice plate substructure described above and which is typical in sea ice (Fig. 3h). Regular elongated protu-

berances appear at the ice-water interface during ice growth and salts are present as liquid inclusions trapped along these substructure (Lofgren and Weeks, 1969).

Comparison of ionic profiles with the isotopic ones, raises the question of the lack of symmetry between them. One could indeed expect the latter be a mirror image of the former, since on the one hand ions are expelled from the growing solid phase and on the other hand heavy isotopes are preferentially incorporated in the growing ice. In fact we observe different situations. Firstly the "end of reservoir" effect appears higher in the profile for isotopes than for ions. Secondly the isotopic enrichment detected between 230 and 256 cm depth has no counterparts on the ionic profile. These differences can be explained as follows. The isotopic profile mainly describes the isotopic composition of the ice lattice of the crystals whereas the ionic profile mainly describes the brines present at the grain boundaries. Because the ice crystals are large in the studied core, the samples taken for ionic analyses have intersected only a small number of crystal boundaries where the brines are located. On the contrary, within the deepest 10 cm, as indicated above, the ice crystals are much smaller and the crystal boundaries intercepted more numerous.

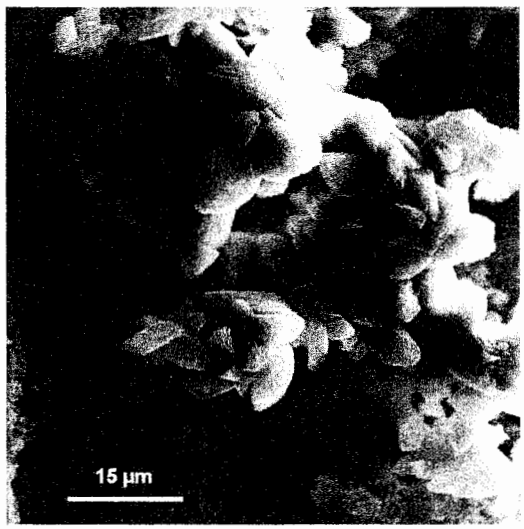

FIGURE 5. SEM photograph of calcium carbonate precipitate from the particles in the ice from the very bottom of the studied core. Calcite crystals appear as scalenohedrons showing growth patterns, for instance in the upper right part of the picture.

GAS DATA

Results of the gas analyses give support to the interpretation of the other data. The gas total content is very low compared to values typical of polar meteoric ice, which is about 0.1 $cm^3\ g^{-1}$ of ice at standard temperature and pressure conditions (Martinerie et al., 1992). The values obtained from our samples are around 0.02 $cm^3\ g^{-1}$ with one exception near the bottom of the core where there is a maximum of 0.08 $cm^3\ g^{-1}$. These values are, however, higher than the normal gas content of bubble-free ice which usually is less than 0.00003 $cm^3\ g^{-1}$ (Berner et al., 1977). By comparison, the solubility of air in water at 0°C is about 0.03 $cm^3\ g^{-1}$. Experiments of downward growth of ice from dilute solutions in a closed reservoir were carried out by Killawee et al. (1998). Some of these, conducted at constant linear rates of about 0.8 µm s^{-1} have lead to interesting conclusions which are relevant to our results. For instance, they have produced total gas contents reaching values between 0.05 and 0.06 $cm^3\ g^{-1}$ in their later stages, i.e., in the ice formed when the freezing front was approaching the bottom of the reservoir. Vertical trains of bubbles were observed and have been interpreted to be due to repeated nucleation of bubbles from particular points at the bottom of the reservoir. They are very similar to some observed in deep parts of our ice core (Fig. 3).

Our results thus again reflect the progressive freezing from top to bottom of the lake water mass. During this process, gases become supersaturated in the region immediately below until bubbles nucleate and form a gas phase. As freezing proceeds, gas is transferred from solution to the bubbles until finally the bubbles are entrapped in the ice (Craig et al., 1992).

The measured CO_2 concentration is higher than the present day atmospheric value all along the core (ranging from 564 to 4557 ppmv) but at the bottom it reaches the exceptionally high level of 695,000 ppmv which to our knowledge is the highest value ever reported for natural ice. Until now, the highest published values were 222,000 ppmv in the basal ice of Suess Glacier (Lorrain et al., 1999) and 135,000 ppmv in the basal ice of the GRIP core in Central Greenland (Souchez et al., 1995). In the experiments of Killawee et al. (1998) cited above, CO_2 contents commonly reached 30%. In one of them, where the rate of freezing was about 2.2 µm s^{-1} and the calcium concentration of the ice from the last freezing stages was about 1.3 mmol L^{-1}, the CO_2 content peaked at about 63% (630,000 ppmv), which is close to our value of 695,000 ppmv obtained at the very bottom of the core. This experiment showed that this very high CO_2 concentration (much higher than the CO_2 concentration in air dissolved in water at 0°C and at atmospheric pressure) is explained by the addition of CO_2 produced by $CaCO_3$ precipitation ($Ca^{2+}_{(aq)} + 2\ HCO_{3\ (aq)} \rightarrow CaCO_{3\ (s)} + H_2O_{(aq)} + CO_{2\ (aq\ or\ gas)}$) and, indeed, calcite crystals were found within the ice produced in the last freezing stages.

In our case, the calcium concentration of the deepest ice samples of the core (2.187 mmol L^{-1}) is even higher than the values of the experiment reported above (1.3 mmol L^{-1}). This process of CO_2 enrichment is thus highly probable in the context of calcite precipitation in a eutectic calcite-ice-aqueous solution as described by Hallet (1976). The particle content of the ice from the very bottom of the core has been investigated by scanning electron microscopy. Calcite precipitates have been detected (Fig. 5) confirming the occurrence of the described process. Concentration of solutes by freezing thus leads to an increase in pCO_2 and supersaturation for calcite at the ice-water interface. When the solution becomes highly supersaturated for calcite, precipitation occurs and is associated with degassing of bubbles containing over 50% CO_2 which become trapped in ice.

BUILD-UP OF THE ICE COVER

From the different aspects of the ice study developed above, it clearly appears that the ice retrieved from the "ice-block" Lake Popplewell has built up from a closed or quasi-closed water reservoir by progressive downward freezing until the lake bottom has been reached. However, no time scale can be provided. It is well known that a water body in contact with the atmosphere at this locality can form an ice cover about 3 m thick over the first year of its existence (Chinn, 2001), but this does not help in this case. Indeed, due to superficial ablation, the 3.3 m thick ice we have sampled does not correspond necessarily to the whole thickness formed since the beginning of the process. This process may have lasted several

years, so long as moat water has not been in contact with the water remaining at the bottom of the central part of the lake (except, as discussed above, when the ice between 230 and 256 cm deep formed). As pointed out by Chinn (1993), both the lake levels in the Dry Valleys and the equilibrium thickness of the ice covers have always fluctuated substantially. We think that during the history of the glacier-dammed lake, a floating ice cover eventually grounded, except in the deeper central part of the lake, and that the climatic conditions allowed thickening of the ice until the bottom was reached in that part. The ice studied here was formed after the grounding event, probably due to a lowering of the lake level.

Following Chinn (1993), the dry-based lakes of the Dry Valleys have a thermal behavior similar to that of glacier ice, with limited upward heat flow because, in contrast to what happens in wet-based lakes, once the lake has completely frozen, there is no further latent heat supply from freezing at the base. Once a lake becomes dry based, it is unlikely for it to return to an ice-covered lake of water if the climate remains constant. A dry-based lake is fed only by flooding over the ice surface of glacier- or snowbank meltwater. The surficial alimentation-ablation balance governs the ice thickness. In the case of Lake Popplewell, a small stream which sporadically flows along the right side of Suess Glacier during the most sunny days of summer, eventually reaches the moat. On very rare occasions, this stream floods. As a result, a sheet of water spills on the ice cover of the lake and freezes on. The icings (aufeis) which are formed by this process are responsible for the bluish smooth surface of the ice cover. Some of us observed one of these phenomena in progress during the 1997–98 summer; in about 5 d, an icing, a few centimeters thick, froze completely solid on most of the surface of the lake ice.

Significantly, we do not find any trace of aufeis in any of the ice cores retrieved from the lake. Aufeis is usually laminated (Schohl and Ettema, 1986) and is generally characterized by small equigranular crystals that do not show discernible structure or *c*-axis orientation patterns (Pollard and van Everdingen, 1992). Moreover, aufeis presents a specific isotopic signature: absence of correlation between δ and deuterium excess (d) values (Souchez et al., 2000). This is the opposite of what we observe here (see description of ice crystals above and Fig. 2b, c showing a clear δD-d relationship). We interpret the absence of visible aufeis as follows. On a mean annual basis, the icings are counterbalanced by the surface ablation loss, which ranges between 0.200 and 0.305 m yr^{-1} (Chinn, 1993). However, Lake Henderson (also called Mummy Pond—see Fig. 1), which is located a few hundred meters westward of Lake Popplewell and is also dry based, has been reported as slightly rising (a few decimeters) between 1972 and 1990 (Chinn, 1993). Lake Popplewell should also have risen since it most probably behaves like its close neighboring Lake Henderson. We think that aufeis is probably present on top of the studied mass but has not been noticed because it corresponds to the top 35 cm which were discarded during sampling since it was extremely brittle, as indicated above.

GLACIER-LAKE INTERACTIONS

Chinn (1993) has extensively examined the possible interactions between Dry Valleys lakes and glaciers margins. He has considered configurations generated by equilibrium, advance or retreat of the glaciers and by static, rising or falling lake levels. Situations like lake ice moving over glacier ice or glacier ice extending out over lake ice are possible and point to the complexity of what can be found at the glacier base. In the present case, basal ice of the damming Suess Glacier has already been investigated (Lorrain et al., 1999). Although this glacier is cold-based (temperature lower than −17°C), it shows some blocks of undisturbed lacustrine sediments within its basal part. The latter consists of a 3- to 5-m-thick series of ice layers of variable thickness (1 cm to a few decimeters), interbedded with sand and fine gravel beds. Occasionally a thin organic mud layer or an algae layer (a few millimeters thick) is associated with a sand layer. The particle-size characteristics of the sediments are the same as those of the adjacent lacustrine environment (Fitzsimons, 1996). The well-preserved primary sedimentary structures of the blocks cited above suggest the sediments were frozen during entrainment. The analyses of stable isotopes and of gas content and composition of this basal ice have indicated that these blocks were formed by the freezing of water. The 85 ice samples taken from this basal ice have isotopic values ranging from −28.10 to −38.64‰ in $\delta^{18}O$ and −228.5 to −286.8‰ in δD. In a δD-$\delta^{18}O$ diagram, they show a regression line having the equation:

$$\delta D = 5.4\ \delta^{18}O - 79\ (r^2 = 0.97) \quad (5)$$

which is practically the same as equation (1) obtained from the lake ice samples presented above. The gas analyses also have shown clear similarities with what is reported here for lake ice: low total gas content (0.006 to 0.083 $cm^3\ g^{-1}$) high to very high CO_2 concentrations (446 to 222,900 ppmv) and O_2/N_2 ratios ranging from 0.25 to 0.52.

From these results Lorrain et al. (1999) concluded that the basal ice of Suess Glacier has been formed by freezing of water from the lake. It is now established that Lake Popplewell no longer has liquid water at its bottom. It is possible that the basal ice investigated has partly been formed by incorporation of lake ice at the glacier base, as in one of the situations envisaged by Chinn (1993). It is nevertheless a fact that some of the ice layers present in the basal ice of Suess Glacier confirm the local freezing of liquid water pockets. For instance, Figure 6 shows the variation of the isotopic composition in δD and $\delta^{18}O$ of one of these ice layers about 13 cm thick situated at the bottom of the basal ice sequence. One can observe isotopic shifts from −29.32 to −37.57‰ in $\delta^{18}O$ and from −238.0 to −284.2‰ in δD which are nearly as large as what is observed through the whole thickness of the lake ice cover. Moreover, when plotted on a δD-$\delta^{18}O$ diagram (Fig. 6), these isotopic values show a linear regression line with the equation

$$\delta D = 5.6\ \delta^{18}O - 72\ (r^2 = 0.99) \quad (6)$$

which again is almost the same as equations (1) and (5). The fact that the isotopic shifts are nearly the same (in value and in range) as in the lake, but displayed on a very small thickness (about 12 cm) indicates that a water pocket of nearly the same isotopic composition as the lake water has frozen completely from both directions. This interpretation is reinforced by the fact that the CO_2 composition varies from 1177 ppmv at one side to 11,306 ppmv in the middle. The isotopic and gas characteristics are not compatible with what should be observed within a slab of lake ice about 12 cm thick incorporated solid at the glacier sole. In this latter case indeed, only a small isotopic shift would be displayed within a decimeter thick ice layer. Here the mean isotopic gradient in δD is about 8‰ cm^{-1} whereas the highest gradient within the lake ice studied is about 0.8‰ cm^{-1}. Moreover, similar isotopic shifts and gradients have been encountered higher up in the basal ice sequence, 35, 270, and 290 cm above the ice layer described here in detail. The corresponding isotopic

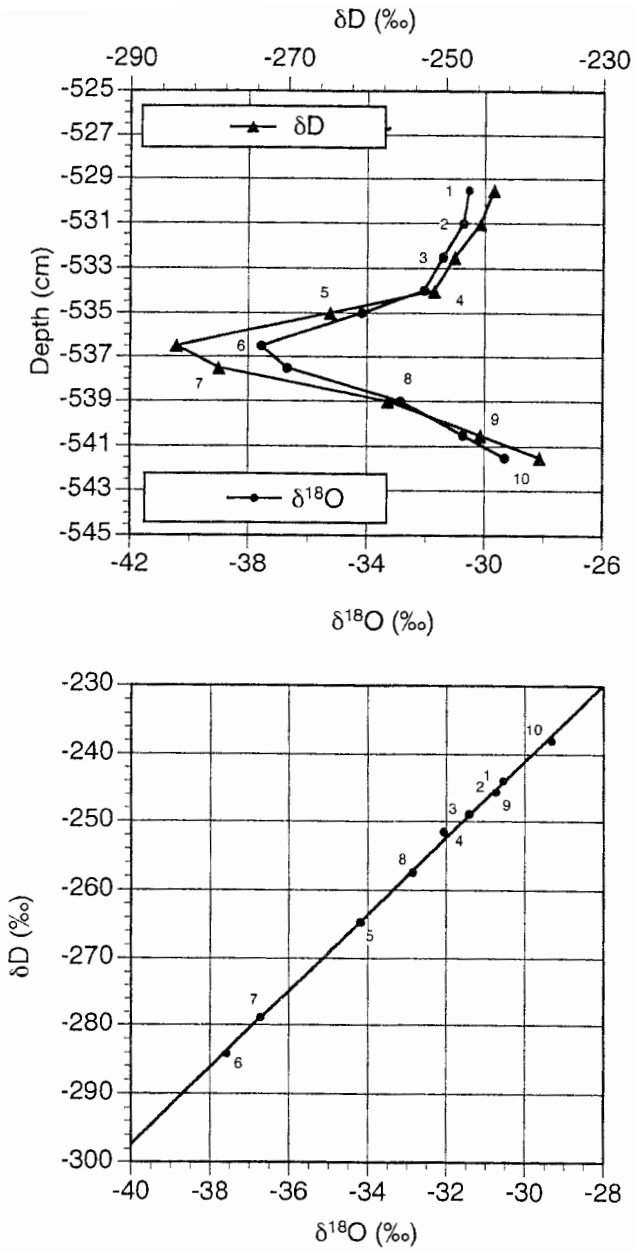

FIGURE 6. δD and $\delta^{18}O$ diagram and profiles of one of the ice layers present in the basal part of Suess Glacier front.

shifts are 40.7, 22.5, and 39.5‰ in δD and their gradients are about 9, 4, and 4‰ cm^{-1}, respectively. These ice layers, some of which containing sediment layers and algae fragments, clearly also result from freezing of liquid water of similar initial isotopic composition.

Pockets of lake water can be present at the glacier base if the glacier flows into a wet-based lake. The model proposed by Fitzsimons (1996) and confirmed by Lorrain et al. (1999), suggests that transient wet-based conditions can occur as the glacier flows onto the unfrozen sediments of the lake bottom, creating conditions favorable for the entrainment of sediments and organic debris and for ice accretion by water freezing. In the case of Suess Glacier, the isotopic data are compatible with that process. It is probable that the stacked sequence of ice and sediment layers accreted at the base and visible at the glacier front has been formed when Lake Popplewell was still wet-based.

Conclusion

Isotopic analyses (in δD and $\delta^{18}O$) of the ice of Lake Popplewell together with ionic and gas data strongly suggest that this ice-block lake has been formed by progressive freezing from top to bottom of the closed water reservoir remaining in the deepest part of the lake after the grounding of a floating ice cover probably due to a lowering of the lake level. This study confirms that the basal ice sequence, visible at the front of Suess Glacier, has been built up, at least partly, by freezing of bottom water from Lake Popplewell in a period during which the lake was wet-based.

Acknowledgments

We want to thank Antarctica New Zealand for providing the logistical support for this study as well as the Marsden Fund and the University of Otago for financial support. We also thank M. Vandergoes and K. Sinclair for assistance with the fieldwork, Dr. A. Bernard for SEM investigations and Dr. R. Souchez and Dr. J.-L. Tison for their constructive comments on an early draft of this paper. This paper is a contribution to the Belgian Scientific Program on Antarctica (Science Policy Office). We are also indebted to Dr. T. Chinn and to an anonymous referee for their helpful critical comments.

References Cited

Adams, E. E., Priscu, J. C., Fritsen, C. H., Smith, S. R., and Brackman, S. T., 1998: Permanent ice covers of the McMurdo Dry Valleys lakes, Antarctica: bubble formation and metamorphism. *In* Priscu, J.C. (ed.), *Ecosystem Dynamics in a Polar Desert, the McMurdo Dry Valleys, Antarctica.* Antarctic Research Series, 72. Washington, D.C.: American Geophysical Union, 281–295.

Barnola, J. M., Raynaud, D., Neftel, A., and Oeschger, H., 1983: Comparison of CO_2 measurements by two laboratories on air from bubbles in polar ice. *Nature,* 303: 410–413.

Berner, W., Bucker, P., Oeshger, H., and Stauffer, B., 1977: Analysis and interpretation of gas content and composition in natural ice. *IAHS—AISH Publication,* 118: 272–284.

Blunier, T., Chappellaz, J. A., Schwander, J., Barnola, J., Desperts, W., Stauffer, B., and Raynaud, D., 1993: Atmospheric methane record from a Greenland ice core over the last 1000 years. *Geophysical Research Letters,* 20: 2219–2222.

Chinn, T. J., 2001: Personal Communication. National Institute of Water and Atmosphere, P.O. Box 6414, 709 Great King Street, Dunedin, New Zealand.

Chinn, T. J. and Maze, I., 1983: *Hydrology and Glaciology, Dry Valleys, Antarctica.* Christchurch: New Zealand Ministry of Works and Development. 64 pp.

Chinn, T. J. H., 1993: Physical hydrology of the Dry Valleys lakes. *In* Green, W. J. and Friedmann, E. I. (eds.), *Physical and Biogeochemical Processes in Antarctic Lakes.* Antarctic Research Series, 59. Washington, D.C.: American Geophysical Union, 1–51.

Craig, H., Wharton Jr., R. A., and McKay, C. P., 1992: Oxygen supersaturation in ice-covered Antarctic lakes: biologic versus physical contributions. *Science,* 255: 318–321.

Fitzsimons, S. J., 1996: Formation of thrust-block moraines at the margins of dry-based glaciers, south Victoria Land, Antarctica. *Annals of Glaciology,* 22: 68–74.

Fritsen, C. H., Adams, E. E., McKay, C. P., and Priscu, J. C., 1998: Permanent ice covers of the Mc Murdo Dry Valleys lakes, Antarctica: liquid water contents. *In* Priscu, J. C. (ed.), *Ecosystem Dynamics in a Polar Desert, the McMurdo Dry Valleys, Antarctica.* Antarctic Research Series, 72. Washington, D.C.: American Geophysical Union, 269–280.

Gow, A. J., Ackley, S. F., Buck, K. R., and Golden, K. M., 1987:

Physical and structural characteristics of Weddell Sea pack ice. *US Army CRREL Report,* 87-14. 70 pp.

Gow, A. J. and Langston, D., 1977: Growth history of lake ice in relation to its stratigraphic, crystalline and mechanical structure. *US Army CRREL Report,* 77-1. 24 pp.

Green, W. J. and Friedmann E. I., (eds.), 1993: *Physical and Biogeochemical Processes in Antarctic Lakes.* Antarctic Research Series, 59. Washington, D.C.: American Geophysical Union. 369 pp.

Hallet, B., 1976: Deposits formed by subglacial precipitation of $CaCO_3$. *Geological Society of America Bulletin,* 87: 1003–1015.

Jouzel, J. and Souchez, R., 1982: Melting-refreezing at the glacier sole and the isotopic composition of the ice. *Journal of Glaciology,* 28(98): 35–42.

Killawee, J. A., Fairchild, I. J., Tison, J.-L., Janssens, L., and Lorrain, R., 1998: Segregation of solutes and gases in experimental freezing of dilute solutions: Implications for natural glacial systems. *Geochimica et Cosmochimica Acta,* 62: 3637–3655.

Lofgren, G. and Weeks, W. F., 1969: Effect of growth parameters on the substructure spacing in NaCl ice crystals. *Journal of Glaciology,* 8(52): 153–164.

Lorrain, R. D., Fitzsimons, S. J., Vandergoes, M. J., and Stiévenard, M., 1999: Ice composition evidence for the formation of basal ice from lake water beneath a cold-based Antarctic glacier. *Annals of Glaciology,* 28: 277–281.

Martinerie, P., Lipenkov, V. Y., Raynaud, D., Chappellaz, J., Barkov, N. I., and Lorius, C., 1994: Air content paleo-record in the Vostok ice core (Antarctica): a mixed record of climatic and glaciological parameters. *Journal of Geophysical Research,* 99: 10565–10576.

Martinerie, P., Raynaud, D., Etheridge, D. M., Barnola, J. M., and Mazaudier, D., 1992: Physical and climatic parameters which influence the air content in polar ice. *Earth and Planetary Science Letters,* 112: 1–13.

Matsubaya, O., Sakai, H., Torii, T., Burton, H., and Kerry, K., 1979: Antarctic saline lakes—stable isotopic ratios, chemical compositions and evolution. *Geochemica et Cosmochimica Acta,* 43: 7–25.

Pollard, W. H. and van Everdingen, R. O., 1992: Formation of seasonal ice bodies. *In* Dixon, J. C. and Abrahams, A. D. (eds.), *Periglacial Geomorphology.* The Binghampton Symposia in Geomorphology: International Series, 22. Chichester: Wiley, 281–304.

Priscu, J. C. (ed.), 1998: *Ecosystem Dynamics in a Polar Desert, the McMurdo Dry Valleys, Antarctica.* Antarctic Research Series, 72. Washington, D.C.: American Geophysical Union. 216 pp.

Raynaud, D., Chappellaz, J., Barnola, J. M., Korotkevich, Y. S., and Lorius, C., 1988: Climatic and CH_4 cycle implications of glacial-interglacial CH_4 change in the Vostok ice core. *Nature,* 333: 655–657.

Raynaud, D., Delmas, R., Ascencio, J. M., and Legrand, M., 1982: Gas extraction from polar ice cores: a critical issue for studying the evolution of atmospheric CO_2 and ice-sheet surface elevation. *Annals of Glaciology,* 3: 265–268.

Schohl, G. A. and Ettema, R., 1986: Theory and laboratory observations of naled ice growth. *Journal of Glaciology,* 32(111): 168–177.

Souchez, R. and Jouzel, J., 1984: On the isotopic composition in δD and $\delta^{18}O$ of water and ice during freezing. *Journal of Glaciology,* 30(106): 369–372.

Souchez, R., Jouzel, J., Lorrain, R., Sleewaegen, S., Stiévenard, M., and Verbeke, V., 2000: A kinetic isotope effect during ice formation by water freezing. *Geophysical Research Letters,* 27: 1923–1926.

Souchez, R., Lemmens, M., and Chappellaz, J., 1995: Flow-induced mixing in the GRIP basal ice deduced from the CO_2 and CH_4 records. *Geophysical Research Letters,* 22: 41–44.

Souchez, R. and Lorrain, R., 1991: *Ice Composition and Glacier Dynamics.* Springer Series in the Physical Environment. Heidelberg, New-York: Springer-Verlag. 207 pp.

Stauffer, B., Neftel, A., Oeschger, H., and Schwander, J., 1985: CO_2 concentration in air extracted from Greenland ice samples. *In* Langway, C. (ed.), *Greenland Ice Core: Geophysics, Geochemestry and the Environment,* Washington, D.C.: American Geophysical Union, 85–89.

Stuiver, M., Yang, I. C., Denton, G. H., and Kellog, B., 1981: Oxygen isotope ratios of Antarctic permafrost and glacier ice. *In* McGinnis, L. D. (ed.), *Dry Valley Drilling Project.* Antarctic Research Series, 33. Washington, D.C.: American Geophysical Union, 131–139.

Terwilliger, J. P. and Dizio, S. F., 1970: Salt rejection phenomena in the freezing of saline solutions. *Chemical Engineering Science,* 25: 1331–1349.

Weeks, W. F. and Ackley, S. F., 1986: The growth, structure and properties of sea ice. *In* Untersteiner, N. (ed.), *The Geophysics of Sea Ice.* NATO ASI Series B, Physics. Dordrecht: Martinus Nyhoff, 51–57.

Ms submitted April 2001